



# Influence of the Brønsted acidity, $\text{SiO}_2/\text{Al}_2\text{O}_3$ ratio and Rh–Pd content on the ring opening: Part I. Selective ring opening of decalin



Silvana A. D'Ippolito<sup>a</sup>, Catherine Espel<sup>b</sup>, Laurence Vivier<sup>b</sup>, Florence Epron<sup>b</sup>, Carlos L. Pieck<sup>a,\*</sup>

<sup>a</sup> Instituto de Investigaciones en Catálisis y Petroquímica (INCAPE) (FIQ-UNL, CONICET), Santiago del Estero 2654, 3000 Santa Fe, Argentina

<sup>b</sup> Institut de Chimie des Milieux et Matériaux de Poitiers (IC2MP), UMR 7285, CNRS – Université de Poitiers, 4 rue Michel Brunet, 86022 Poitiers Cedex, France

## ARTICLE INFO

### Article history:

Received 25 February 2013

Received in revised form 5 June 2013

Accepted 16 June 2013

Available online 31 July 2013

### Keywords:

Ring opening

Bronsted acidity

Bimetallic catalysts

Rh–Pd

Bifunctional catalysts

Decalin

## ABSTRACT

The influence of the Brønsted acidity,  $\text{SiO}_2/\text{Al}_2\text{O}_3$  ratio and Rh–Pd content on the ring opening of decalin was studied. Rh- and Pd-based monometallic and bimetallic catalysts were prepared by impregnation on three commercial  $\text{SiO}_2/\text{Al}_2\text{O}_3$  supports (SIRAL 5, 20 and 40). The catalysts were characterized by TPD of pyridine, X-ray diffraction,  $\text{H}_2$  chemisorption, isomerization of 3,3-dimethyl-1-butene (33DM1B) and selective ring opening (SRO) of decalin. It was found that the support acidity is strongly influenced by the  $\text{SiO}_2/\text{Al}_2\text{O}_3$  ratio, the SIRAL 40 being more acid. The metal accessibility has the following order: supported catalysts on SIRAL 40 > SIRAL 20 > SIRAL 5. The incorporation of Rh and/or Pd modifies the conversion and the product distribution on decalin reaction. The support acidity has a strong influence on the conversion and product distribution on the decalin reaction at 350 °C. SIRAL 5 series have low selectivity to RO and high selectivity to dehydrogenated compounds. On the other hand, SIRAL 40 series lead to the highest yield to cracking products of the three studied series. Catalysts with Rh/Pd atomic ratios equal to 2 and monometallic Rh1 supported on SIRAL 40 are the most active and selective catalysts to ring opening products.

© 2013 Elsevier B.V. All rights reserved.

## 1. Introduction

Petroleum refining industry needs more capacity to cope with an increasing demand of high quality fuels, with low aromatic, sulfur and nitrogen content and higher cetane number (CN). CN is the key parameter for diesel fuels to secure a proper combustion quality which leads to a lower level of NOx and particulate matter emissions [1]. The lowering of S and aromatic contents in fuels has been traditionally achieved using well known hydrotreating and hydrocracking technologies [2]. The selective ring opening (SRO) of naphthenic molecules is an alternative route for the valorization of several products resulting from catalytic reforming and cracking processes [3–5], due to the hydrogenation of aromatic compounds followed by a selective opening of the obtained naphthenes to paraffins allowing to improve notably the fuel quality. It is known that normal paraffins increase the CN of fuels [6]. Research works on SRO have mainly dealt with reactions of one-ring molecules despite the fact that two-ring molecules are more

important to diesel chemistry. These are abundant in light cycle oil (LCO), an fluid catalytic cracking (FCC) residue commonly upgraded by hydrotreating in order to contribute to the diesel pool. The SRO of bicyclic naphthenes such as decalin is very important in the processing of LCO; the CN significantly increases when decalin is converted into linear or monobranched paraffins. Two main reaction types occur during the catalytic ring opening (RO) process. A first possible reaction type is the rupture of C–C bonds attached to naphthenic rings, associated with a decreasing in mean molecular weight of products. On the other hand, the main desired reaction, i.e. SRO, does not significantly affect the resulting molecular weight due to the internal nature of C–C ring bonds.

Decalin ring opening reaction can proceed by acid or metal mechanisms as reported in detail by Resasco et al. [7]. On the other hand, Mostad et al. proposed that the decalin cracking is initiated by hydride abstraction [8,9]. The support acidity is particularly important for the opening of compounds having more than one ring, such as decalin [10]. Zeolites are a special kind of useful acid supports for this purpose. Corma et al. studied the conversion of decalin on zeolites of different pore sizes and found that the pore size and channel topology have a strong influence on diffusion and adsorption, and therefore on the product distribution [11]. Zeolites with

\* Corresponding author. Tel.: +54 342 4533858; fax: +54 342 4531068.

E-mail address: [pieck@fiq.unl.edu.ar](mailto:pieck@fiq.unl.edu.ar) (C.L. Pieck).

large-sized pores (USY, beta, mordenites) as ring opening catalysts are more selective to RO products as compared to middle pore size ones; consequently, this parameter is very important in RO catalysis [11]. Zeolites of larger pore size, such as HY, are considered as one of the most appropriate supports for ring opening catalysts [12,13]. The zeolite crystal size [14] and the number and strength distribution of the acid sites [11,15] are important parameters for ring opening activity and selectivity. Kubicka et al. [15,16] found an important influence of acidity in the SRO of bicyclic naphthenes, the presence of Brønsted sites is required for ring opening and isomerization. Santikunaporn et al. [17] studied the contraction and ring opening of decalin and tetralin and found that the Pt/HY catalysts are more effective than HY catalysts without metal promoter. The addition of Pt to USY zeolites was also found to greatly increase the rate of isomerization and therefore the formation of ring opening products. For these bifunctional metal–acid catalysts, the formation of ring opening products increases with the proximity between the Pt and the acid sites and also with the increase of the metal/acid ratio [18].

Amorphous silica–alumina (ASA) may replace advantageously zeolites, which often lead to excessive cracking activity, as carriers for bifunctional metal–acid catalysts. ASA supports contain not only silica–alumina mixed phases, but also pure silica and aluminum clusters [19]. They present strong Brønsted acid sites; with strength comparable to that of zeolites but in much lower concentration, which can be adjusted by varying the silica content [20]. It has been widely reported that the SiO<sub>2</sub> increases acidity of silica–alumina support improving catalyst performance particularly for deep hydrodesulfurization (HDS) of diesel fuel [21]. Nassreddine et al. [22,23] demonstrated that ASA supports provide a good ring-opening and contraction selectivity to iridium for tetralin hydroconversion in the presence of sulfur. It was shown that the most active and selective Ir/ASA catalyst for tetralin conversion was the one with 40% of silica in the support, which presents the highest Brønsted acidity.

In this work, the influence of the Brønsted acidity of the support on the selective ring opening of two-ring naphthenic compounds was studied. Mono and bimetallic Pd–Rh catalysts supported on SiO<sub>2</sub>–Al<sub>2</sub>O<sub>3</sub> with different SiO<sub>2</sub> contents (SiO<sub>2</sub> = 5, 20 and 40 wt%) and different atomic Rh/Pd ratios were used. Decalin was taken as model molecule.

## 2. Experimental

### 2.1. Catalysts preparation

Three commercial SiO<sub>2</sub>–Al<sub>2</sub>O<sub>3</sub> supports provided by Sasol (SIRAL 5, SIRAL 20 and SIRAL 40) were used as support. Previously, they were calcined at 450 °C for 4 h (10 °C min<sup>-1</sup>, air, 60 cm<sup>3</sup> min<sup>-1</sup>). Rh and/or Pd were added by a common impregnation method. An aqueous solution of HCl (0.2 mol L<sup>-1</sup>) was added to the support and the system was left unstirred at room temperature for 1 h. Then an aqueous solution of RhCl<sub>3</sub> and/or PdCl<sub>2</sub> (Sigma–Aldrich) was added in order to have a 1 wt% of total metal charge. For the bimetallic catalyst, the Rh/Pd atomic ratio was  $x=0.5, 1$  and  $2$ . The slurry was gently stirred for 1 h at room temperature and then it was put in a thermostated bath at 70 °C until a dry solid was obtained. The drying was completed in a stove at 120 °C overnight. Finally, the samples were calcined in flowing air (60 cm<sup>3</sup> min<sup>-1</sup>) at 300 °C for 4 h and reduced under flowing H<sub>2</sub> (60 cm<sup>3</sup> min<sup>-1</sup>, 500 °C, 4 h). The monometallic catalysts are named Pd $x$ /Sy or Rh $x$ /Sy, while the bimetallic are named Rx/Sy, where Sy is the support (SIRAL) and y is the weight percentage of SiO<sub>2</sub>. In the case of the bimetallic catalysts, R corresponds to the Rh/Pd atomic ratio and x is the value of this ratio.

### 2.2. Measurement of the Pd and Rh contents

The composition of the metal function was determined by inductively coupled plasma-optical emission spectroscopy (ICP-OES) after digestion in an acid solution and dilution.

### 2.3. Temperature-programmed reduction (TPR)

The tests were performed in an Ohkura TP2002 apparatus equipped with a thermal conductivity detector. At the beginning of each TPR test the catalyst samples were pretreated in situ by heating in air at 400 °C for 1 h. Then they were heated from room temperature to 700 °C at 10 °C min<sup>-1</sup> in a gas stream of 5.0% hydrogen in argon (molar base).

### 2.4. X-ray diffraction

The analysis was performed with a Shimadzu XD-D1 diffractometer. Diffraction patterns were recorded using Cu K $\alpha$  radiation filtered with Ni in the 10–60° range at a scan rate of 2° min<sup>-1</sup>, operating at 30 kV and 40 mA.

### 2.5. H<sub>2</sub> chemisorption

This technique was used in order to estimate the metallic accessibility of the Pd–Rh bimetallic particles on the surface of the catalyst. The sample (100 mg) was reduced at 500 °C (10 °C min<sup>-1</sup>, H<sub>2</sub> 30 cm<sup>3</sup> min<sup>-1</sup>) for 1 h. Then argon (30 cm<sup>3</sup> min<sup>-1</sup>) was made to flow over the sample for 2 h at 500 °C in order to eliminate adsorbed hydrogen. Finally the sample was cooled down to 70 °C in argon and calibrated pulses of H<sub>2</sub> were injected into the reactor (HC1). These pulses were sent until the sample was saturated. After flushing the system with argon during 30 min, a second set of pulses was injected (HC2). The difference HC1 – HC2 allows one to estimate the metallic accessibility considering the stoichiometry between a hydrogen atom and a surface Pd or Rh atom (H/Pd and H/Rh) equal to 1.

### 2.6. Temperature-programmed desorption of pyridine

The amount and strength of the acid sites of the catalysts were assessed by means of temperature programmed desorption of pyridine. An amount of 200 mg of the catalyst to be tested were first immersed in a closed vial containing pure pyridine (Merck, 99.9%) for 4 h. Then the vial was open and excess pyridine was allowed to evaporate in a ventilated hood at room conditions until the surface of the particles was dried. The sample was then loaded into a quartz tube microreactor and supported over a quartz wool plug. A constant flow of nitrogen (40 mL min<sup>-1</sup>) was made to flow over the sample. A first step of desorption of weakly adsorbed pyridine and stabilization was performed by heating the sample at 110 °C for 1 h. Then the temperature was raised at a rate of 10 °C min<sup>-1</sup> to a final value of 700 °C. The reactor outlet was directly connected to a flame ionization detector.

### 2.7. Isomerization of 3,3-dimethyl-1-butene (33DM1B)

The reaction was performed in a microreactor of U shape (length = 20 cm, diameter = 0.6 cm). The feed was generated by passing a nitrogen stream through a saturator contactor containing the liquid reagent and immersed in an ice bath at 0 °C. The catalyst (50 mg) was pretreated in situ by reduction with H<sub>2</sub> (60 cm<sup>3</sup> min<sup>-1</sup>, 450 °C, 1 h). The sample was then cooled in N<sub>2</sub> (30 cm<sup>3</sup> min<sup>-1</sup>) to the reaction temperature, which was changed in order to have small conversion values to avoid secondary reactions. It was fixed at 100, 150 and 200 °C for SIRAL 40, 20 and 5, respectively. Then the feed

**Table 1**

Percentages of Rh and Pd determined by ICP analysis and theoretical values.

Catalyst	Rh theoretical, wt%	Rh by ICP, wt%	Pd theoretical, wt%	Pd by ICP, wt%	Rh/Pd by ICP	Total metal by ICP, wt%
Pd1/S5	–	–	1.00	0.76	–	0.76
Pd1/S20	–	–	–	0.76	–	0.76
Pd1/S40	–	–	–	0.78	–	0.78
R0.5/S5	0.33	0.26	0.67	0.57	0.47	0.83
R0.5/S20	–	0.28	–	0.59	0.49	0.87
R0.5/S40	–	0.26	–	0.54	0.50	0.80
R1/S5	0.49	0.39	0.51	0.36	1.12	0.75
R1/S20	–	0.37	–	0.37	1.03	0.74
R1/S40	–	0.36	–	0.39	0.95	0.75
R2/S5	0.66	0.54	0.34	0.27	2.07	0.81
R2/S20	–	0.59	–	0.29	2.10	0.88
R2/S40	–	0.52	–	0.28	1.92	0.80
Rh1/S5	1.00	0.78	–	–	–	0.78
Rh1/S20	–	0.84	–	–	–	0.84
Rh1/S40	–	0.79	–	–	–	0.79

from the saturator was injected. The reagent partial pressure and flow rate were 20.9 kPa and 15.2 mmol h<sup>-1</sup>, respectively. The products were analyzed with a gas chromatograph connected on-line. The error associated to the test of 33DM1B isomerization was determined by calculating the variance of the conversion in a set of seven experiments (variance = 6.5%).

### 2.8. Selective ring opening (SRO) of decalin

All SRO experiments were performed in a stainless steel, autoclave-type stirred reactor. The reaction conditions were: temperature = 350 °C, hydrogen pressure = 3 MPa, stirring rate = 1360 rpm, volume of decalin = 25 cm<sup>3</sup>, catalyst loading = 1 g. Used decalin had 37.5% cis isomer and a trans/cis ratio of 1.63. It was found that after few minutes the attrition action of the stirrer reduced the catalyst to powdery slurry that after drying would mostly pass through a 200 meshes sieve. With this particle size and the high stirring rate, it was assumed that diffusional limitations to mass transfer were eliminated. This was further confirmed by calculating the Weisz–Prater modulus ( $\Phi = 0.06 \ll 1$ ). A sample was taken at the end of the experiments and it was analyzed using a Shimadzu 2014 gas chromatograph equipped with a capillary column (Phenomenex ZB-5) and a FID. Previous product identification studies were performed by GC–MS in a Saturno 2000 mass spectrometer coupled to a GC Varian 3800 using the same GC column.

## 3. Results and discussion

### 3.1. Rh and Pd contents determined by ICP

**Table 1** shows the atomic Rh/Pd ratios as well as the percentages of Rh and Pd determined by ICP analysis and the theoretical values. It can be seen that the experimental atomic Rh/Pd ratio is practically the same as the theoretical one. However, the amounts deposited are 15–25% lower than the theoretical ones. On the three supports the highest differences are on the monometallic Pd1 and bimetallic R1 catalysts.

### 3.2. Properties of the supports

**Table 2** presents the main characteristics of the support given by Sasol, as well as the total acidity determined by pyridine TPD normalized to SIRAL 5 support. It can be seen that the numbers 5, 20 and 40 are associated to the weight percentage of SiO<sub>2</sub>, SIRAL

40 being the support with the highest content of SiO<sub>2</sub>. The specific surface area and the total acidity increase with the increase of SiO<sub>2</sub> percentage. Thus SIRAL 40 is 14 times more acidic than SIRAL 5, and SIRAL 20 has a medium acidity which is 8 times higher than SIRAL 5.

### 3.3. Support characterization by XRD

The crystallization of amorphous diphasic Al<sub>2</sub>O<sub>3</sub>–SiO<sub>2</sub> calcined at 450 °C has been studied by XRD diffraction, the patterns being shown in **Fig. 1**. The supports display the characteristic spectral profile of an amorphous silica–alumina structure with an amorphous halo present in the  $2\theta = 24^\circ$  [24,25]. This typical halo results from the dispersion of the angles and bond distances between the basic structural units (silicates and aluminates) which destroys the structure periodicity and produces a non-crystalline material. The XRD peaks detected around  $2\theta$  equal to 37.5°, 46° and 67.4° are attributed to  $\gamma$ -Al<sub>2</sub>O<sub>3</sub> [26]. Fierro et al. [27] indicate that diffraction peaks at ca.  $2\theta = 37.5^\circ$ , 39.6° and 45.9° are due to the  $\gamma$ -Al<sub>2</sub>O<sub>3</sub> substrate whereas an amorphous hump at about  $2\theta = 23^\circ$  belongs to amorphous silica [28]. The presence of diffraction peaks of SiO<sub>2</sub> and Al<sub>2</sub>O<sub>3</sub> demonstrate that SiO<sub>2</sub> and  $\gamma$ -Al<sub>2</sub>O<sub>3</sub> exist separately in the studied supports. The X-ray diffraction patterns differ somewhat according to the nature of the support (SIRAL 5, SIRAL 20 or SIRAL 40). For SIRAL 5 (presenting the highest Al<sub>2</sub>O<sub>3</sub> content), the peaks at  $2\theta = 37.5^\circ$ , 46° and 67.4° are clearly observed, while when SiO<sub>2</sub> content is increased (for SIRAL 20 and all the more for SIRAL 40), a noticeable broad hump at  $2\theta = 20$ –30° appears. Similar results were reported by Leyva et al. [29]. It is known that the width of the diffraction peaks depends on the crystal perfection and size. As it grows the average crystal size decreases. A decrease in the SiO<sub>2</sub> percentage in the support from 39.3 to 4.2 wt% promotes a more

**Table 2**

Main characteristics of the silica–alumina supports used in this work.

	SIRAL 5	SIRAL 20	SIRAL 40
Area (m <sup>2</sup> g <sup>-1</sup> )	323	430	514
Loose bulk density (g mL <sup>-1</sup> )	0.52	0.43	0.33
Al <sub>2</sub> O <sub>3</sub> (wt%)	95.8	80.2	60.7
SiO <sub>2</sub> (wt%)	4.2	19.8	39.3
Particle size			
<25 µm (%)	31.3	18.3	26.0
<45 µm (%)	54.0	47.1	54.6
<90 µm (%)	9.4	96.6	96.1
Total acidity (normalized value)	1.00	8.39	14.42

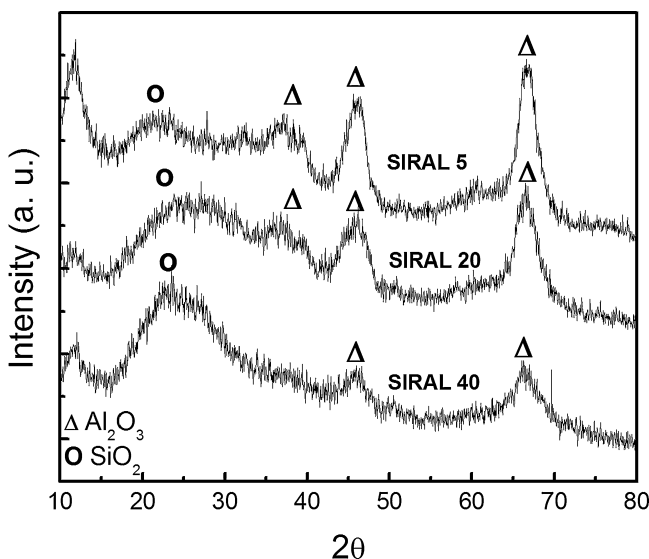


**Fig. 1.** XRD patterns of the supports calcined at 450 °C.

ordered structure. Feng et al. reported that the peaks became wider with increasing  $\text{SiO}_2$  content [30].

### 3.4. Temperature-programmed reduction (TPR)

The results of temperature-programmed reduction (TPR) are not sufficient to determine if the Rh and Pd metals formed an alloy. However this technique can provide information about the interaction between the metal components. The temperature of the peaks of hydrogen consumption and the number of them depend on the oxidation state of the metals, the interaction between the metal oxides and of the metal oxides with the support and on the

possible catalytic action of one metal over the other. **Fig. 2** shows the TPR traces of a series of metals supported on SIRAL 40.

The reduction of Pd oxides at 111 °C on monometallic Pd1 occurs at a lower temperature than the reduction of Rh oxides of monometallic Rh1 catalyst supported on SIRAL 40 (145 °C). Some authors found that the reduction peaks of the Pd species are followed by a negative peak, which is attributed to the release of  $\text{H}_2$  resulting from the decomposition of Pd hydride [31,32]. The palladium crystallites would first be reduced, then a PdH phase would be formed and finally this phase is decomposed with hydrogen release (at about 113 °C) [33]. Other peaks regularly found at room temperature and assigned to a reduction of large Pd-oxide species [34] could not be found in our TPR results. Feio et al. [35] report that this peak is independent of the support composition. According to the literature, calcined monometallic Pd catalysts have a reduction peak at 18 °C attributed to the reduction of crystalline  $\text{PdO}$  to  $\text{Pd}^0$  [36], and a peak at 110 °C, related to the reduction of smaller  $\text{PdO}$  particles interacting with the support. The negative peak attributed to the decomposition of the  $\beta\text{-PdHx}$  phase cannot be distinguished in the TPR trace because it is merged with the 111 °C peak. The same behavior has been reported by Rodríguez et al. [37]. The interaction between the Pd particles and the support is high in the case of Pd1/S40, probably because of the presence of small  $\text{PdO}$  particles strongly interacting with the support and thus resulting in a higher reduction temperature. The R0.5/S40 catalyst shows a main reduction peak at 182 °C and a shoulder at 110 °C. The R1/S40 catalyst has a main reduction peak at 172 °C and a small shoulder at 120 °C. Finally the R2/S40 catalyst has a single reduction peak at 158 °C. It is clear that the bimetallic catalysts supported on SIRAL 40 have a greater interaction with the support than the monometallic catalysts. Also Pd and Rh oxides seem harder to reduce than the Pd species. The R2 bimetallic catalyst has only one reduction peak indicating that Rh and Pd are reduced simultaneously due to a strong Rh–Pd interaction. It can be concluded that in the case of the bimetallic catalysts the interaction between the metals increases with the Rh content.

### 3.5. Hydrogen chemisorption

The hydrogen chemisorptions were performed in order to obtain the metal accessibility ( $\text{H}/(\text{Rh} + \text{Pd})$ ) of the catalysts. It can be seen in **Fig. 3** that the dispersion values are between 30 and 50% for all the studied catalysts. Monometallic Pd catalysts present higher

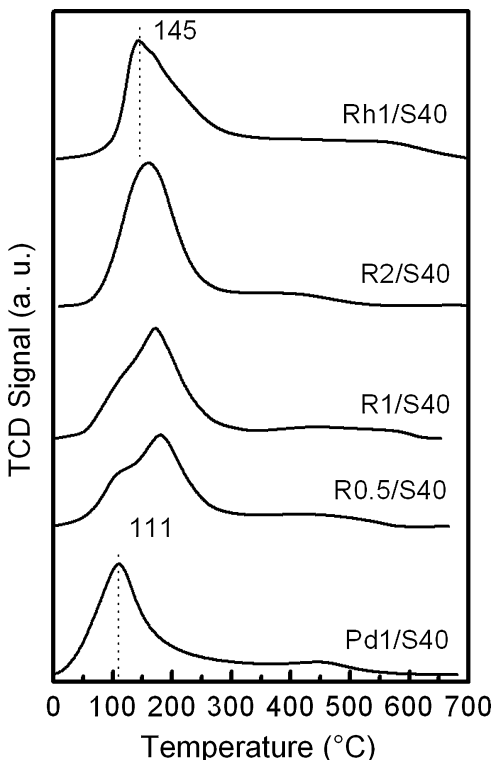


**Fig. 2.** TPR profiles of catalysts supported on SIRAL 40.

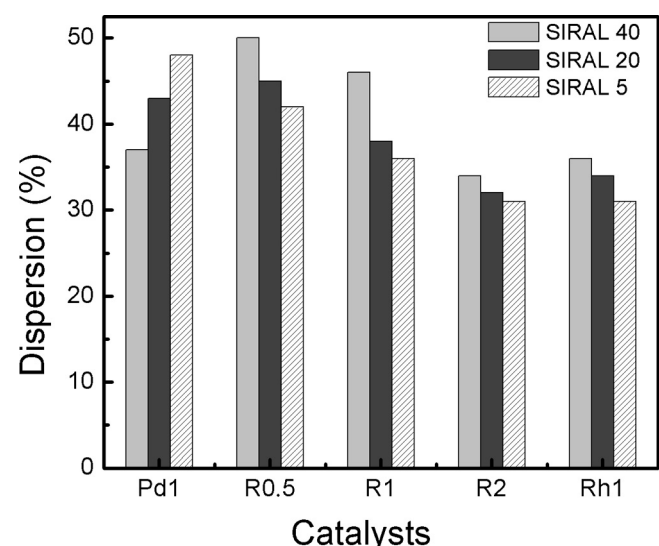


**Fig. 3.** Metallic dispersion of the catalysts obtained by hydrogen chemisorption.

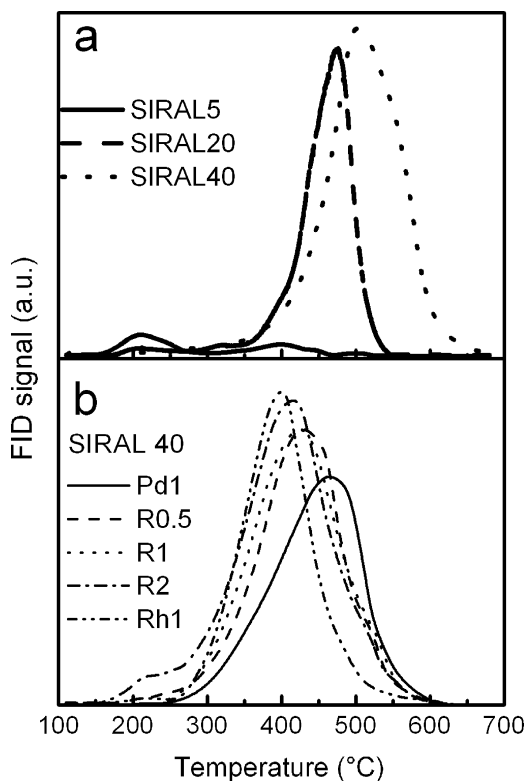


**Fig. 4.** Temperature programmed desorption of pyridine: (a) SIRAL supports and (b) catalysts supported on SIRAL 40.

metallic dispersions than the monometallic Rh ones. The metallic dispersion decreases as the Rh content increases for the three bimetallic series. In general, for the same Rh/Pd ratio, the dispersion is increased as the specific surface area of the support is increased, i.e. in function of the SiO<sub>2</sub> percentage (Table 2). However, the Pd1 catalysts have an opposite behavior.

### 3.6. Total acidity

The profiles of pyridine desorption give information on the acid sites distribution. Fig. 4a shows that SIRAL 40 is the most acid of the three supports and the sites are strongest, due to the higher temperature (503 °C) of the desorption peak. SIRAL 20 presents a desorption peak with a maximum at 475 °C while SIRAL 5 has two small desorption peaks at 212 and 400 °C. The effect of the metallic charge on the acidity of SIRAL 40 can be seen in Fig. 4b. It can be observed that after Rh and Pd addition the total acidity of the support increases due to the effect of Cl<sup>-</sup> ions added, either by the Pd and Rh chlorinated precursors and/or by the added HCl for metal impregnation. On the other hand, the incorporation of metals decreases the strength of the acid sites (desorption peak are shifted to lower temperatures). This effect is more noticeable as rhodium content increases. Such changes in acidity can be attributed to the electronic interactions of the metal particles with the support. Several authors reported the same behavior [38–46] highlighting the redistribution of the acid sites.

### 3.7. Brønsted acidity measured by 33DM1B isomerization

The conversion of the isomerization reaction of 33DM1B was taken as a measure of the concentration of Brønsted acid sites. Kemball et al. [47,48] demonstrated that the Lewis acid sites are not involved in this reaction. 33DM1B isomerization occurs through a protonic mechanism [49–51], where the formation of a secondary

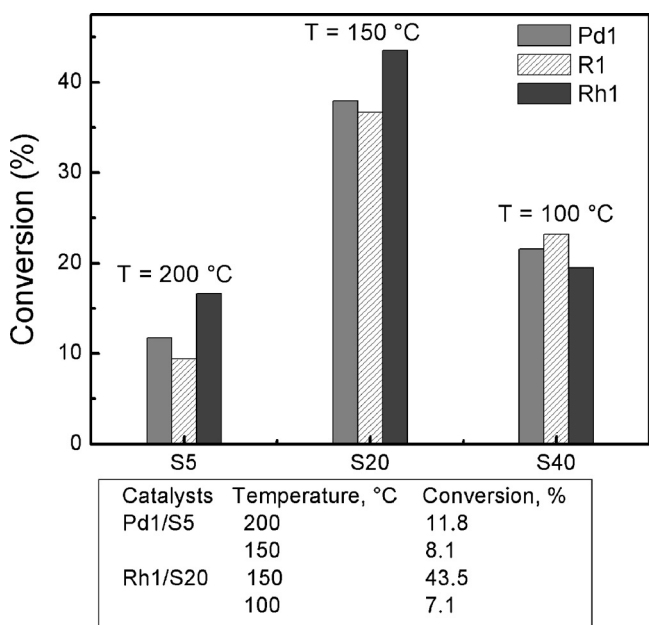


**Fig. 5.** Conversion of 33DM1B extrapolated to zero time reaction.

carbocation leads to the production of two isomers: 2,3-dimethyl-2-butene (23DM2B) and 2,3-dimethyl-1-butene (23DM1B). Other weaker products attributed to methylpentenes appear at higher reaction temperatures (>300 °C) [52]. The maximum reaction temperature used was 200 °C as a consequence in all the experiments the selectivity was 100% to 23DM1B and 23DM2B, demonstrating that the reaction only occurs on the Brønsted acid sites of the support. The reaction was performed at different reaction temperatures according to the support acidity in order to obtain low reaction rates avoiding diffusional and deactivation problems. Fig. 5 shows the conversion extrapolated at zero reaction time for the monometallic and R1 bimetallic catalysts as well as complementary data to justify the temperatures used. It is important to point out that the differences between catalysts of each series are very difficult to infer because the experimental error is 6.5%. The catalysts supported on SIRAL 5 have lower conversions despite of the higher reaction temperature used. Nevertheless, Pd1/S5 at 150 °C (temperature used to evaluate the catalysts supported on SIRAL 20) has a conversion value of 8.1%, which is logically lower than 11.8% obtained at 200 °C. The catalysts supported on SIRAL 20 at 150 °C have higher conversions than the catalysts supported on SIRAL 40 evaluated at 100 °C. However, the Rh1/S20 catalyst which has the maximum conversion value of the series (43.5% at 150 °C) decreased to 7.1% at 100 °C. This is almost three times lower than 19.5% obtained for the Rh1/S40 catalyst which presents the lowest value of the SIRAL 40 series. Therefore, it can be concluded that the amount of Brønsted sites follows the order: S40 > S20 > S5. Similar tendency were reported by Daniell et al. [53] for the SIRAL supports.

Fig. 6 shows the conversion values obtained in the reaction of isomerization 33DM1B as a function of the time for all the catalysts supported on SIRAL 40. The R2/S40 catalyst displays the highest conversion and stability of the series. It is important to note that the metal content does not change significantly the conversion value. The results reported in Fig. 5 and 6 allow establishing that the Brønsted acidity depends strongly on the support and is affected to a lesser degree by the metal content.

### 3.8. Decalin ring opening reaction

Figs. 7 and 8 show the percentage of cis and trans decalin obtained after 6 h of reaction at 350 °C. Higher trans/cis decalin

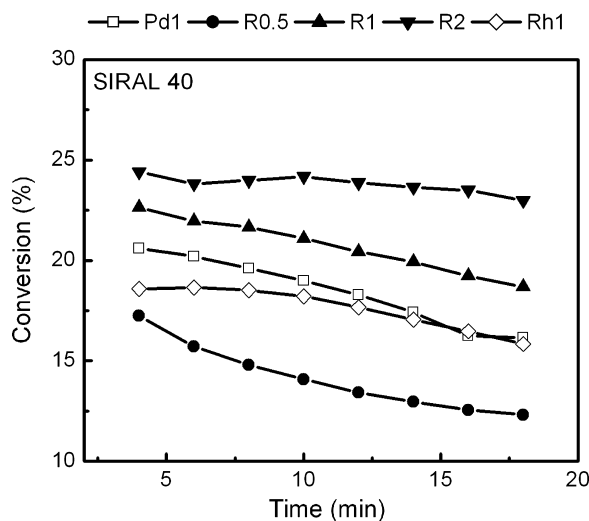


Fig. 6. Conversion of 33DM1B as a function of time for the catalysts supported on SIRAL 40.

ratios than the initial one (1.63) could be due to a higher reactivity of the cis isomer [17,54] and also to the catalytic cis/trans isomerization reaction [55]. Cis-decalin is more selectively converted to RO products than trans-decalin, which is converted mainly to cracking products [17]. Almost for all the catalysts (except Pd1/S20 and R0.5/S20 catalysts) the ratio trans/cis decalin increases as increases the conversion. These results are in agreement with those reported by Lai et al. [56] and Moraes et al. [57]. The catalysts supported on SIRAL 40 have higher trans/cis ratios than the catalysts supported on S20 and S5. It can be seen in Fig. 7 that the support SIRAL 40 is more active than SIRAL 20. The SIRAL 5 produces a trans/cis decalin ratio similar to that of the decalin used as reactive (1.63) since it is not able to convert decalin. The highest conversion of decalin, and consequently the highest activity for decalin conversion, is obtained with the monometallic Rh1 series. The monometallic Rh1 catalysts have higher activity than the corresponding Pd1 catalysts. In agreement with this observation, in the case of bimetallic catalysts, the increase in the Rh content leads to more active catalysts, as it can be seen in Fig. 8, but the Rh1 catalyst is more active than the bimetallic ones.

For the supports alone as well as for the supported mono and bimetallic catalysts, the values of conversion and trans/cis decalin ratio correlate with the acidity order; the catalysts with the most acidic supports show the highest activity and hence the lowest percentage of unreacted decalin and the highest product trans/cis ratio. However, the metal charge has an influence, Rh being more active than Pd in the three series studied.

In each of the bimetallic catalysts series, the increase of the decalin conversion is related to the increase of Rh content, even if the metal dispersion decreases as the Rh content increases. As Rh1 catalysts are more active than the bimetallic ones with the highest Rh content, R2, and the dispersion of Rh1 is slightly superior to that of R2, it can be inferred that the Rh content plays a more significant role than the metal dispersion on the activity of the catalyst.

The yields to different reaction products after 6 h of decalin transformation at 350 °C are presented in Fig. 9. As decalin conversion leads to a complex mixture of more than 200 compounds, the decalin reaction products were classified according to the same criterion used in previous work [58]. The products of reaction are lumped as: cracking products ( $C_1-C_9$  products); ring opening (RO)  $C_{10}$  products; ring contraction (RC) products; naphthalene and other products including heavy dehydrogenated products (DH).

It can be seen in Fig. 9 that the catalysts supported on SIRAL 5 are not adequate for ring opening of decalin because the main reaction products results from dehydrogenation (naphthalene and others). The activity is increased significantly with the Rh content on SIRAL 5. The catalysts supported on SIRAL 5 have the lower acidity of the three series studied, and the support alone is not able to convert decalin at all. As a consequence the metallic function would more influence the products distribution than the acid function, i.e., it is expected that the product distribution depends not only on hydrogenolysis reaction but also on dehydrogenation reaction due to the high reaction temperature (350 °C). It is known that Rh is much more active for the hydrogenolysis reaction than Pd [59], whereas Pd is mainly active for hydrogenation/dehydrogenation reactions. The conversion (Fig. 8) and the yield to dehydrogenated compounds (Fig. 9) increase with the Rh content. For the SIRAL 5 (S5) series, the highest conversions and yields for naphthalene and others are obtained with R1/S5. As for the S5 series only dehydrogenated products are formed, it can be inferred that Rh is much more active for the dehydrogenation of decalin than Pd, and neither Rh nor Pd is able to open or isomerizes this bicyclic.

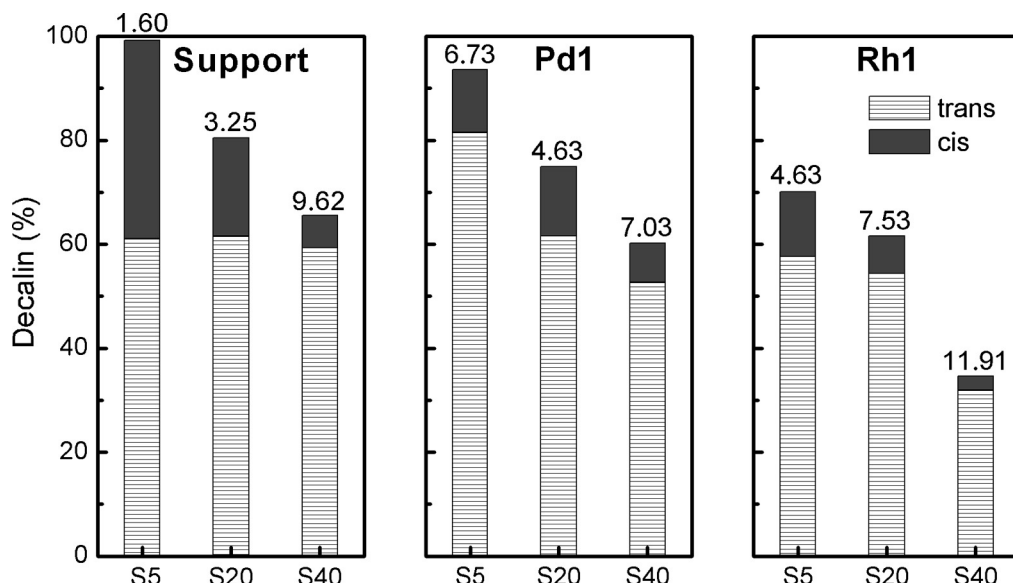
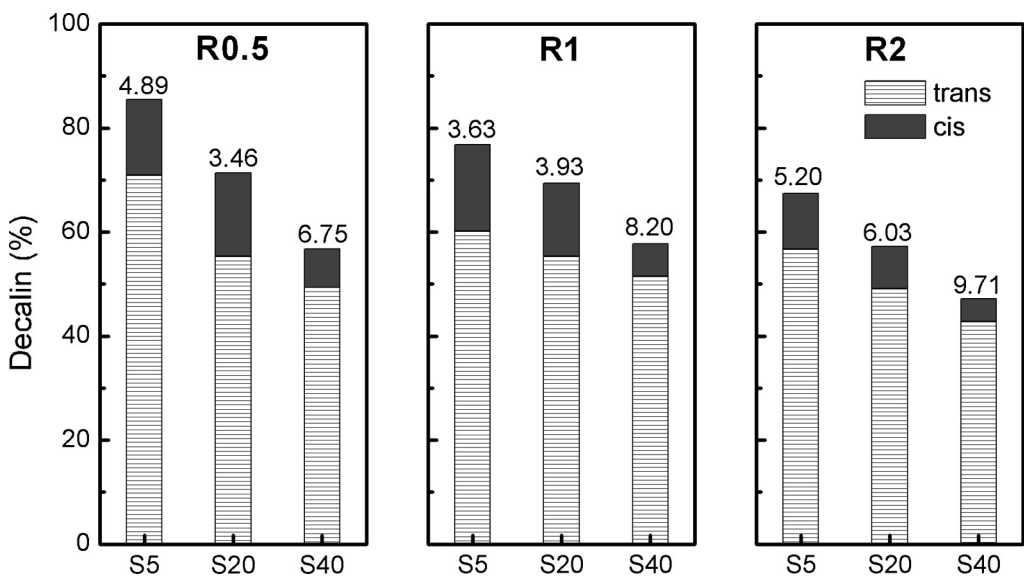
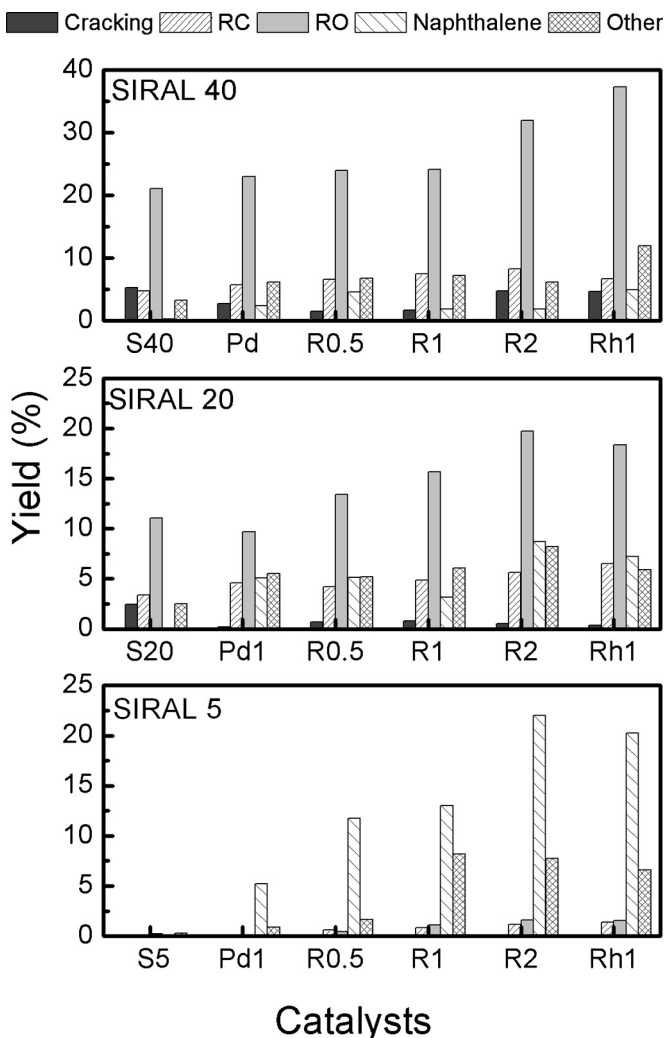


Fig. 7. Trans and cis decalin obtained after 6 h reaction time ( $T_{\text{reaction}} = 350^{\circ}\text{C}$ ) on the supports and monometallic catalysts. Numbers are the trans/cis decalin ratios.



**Fig. 8.** Trans and cis decalin obtained after 6 h reaction time ( $T_{\text{reaction}} = 350^{\circ}\text{C}$ ) on bimetallic catalysts. Numbers are the trans/cis decalin ratios.



**Fig. 9.** Yield at 6 h of decalin transformation divided in cracking products, ring contraction (RC), ring opening (RO), naphthalene and others (heavy dehydrogenated products);  $T_{\text{reaction}} = 350^{\circ}\text{C}$ .

The best performances are obtained with catalysts supported on SIRAL 40 followed by the series supported on SIRAL 20. These results are in agreement with the highest total acidity and the highest Brønsted acidity of the S40 series. The support is very important for the formation of RO products on SIRAL 40 and 20. Although the SIRAL 20 and SIRAL 40 supports alone have activity in decalin opening, the performances can be enhanced by metal addition, notably with the use of bimetallic catalysts with high Rh contents (R2) and monometallic Rh catalysts (Rh1), due to a better balance of metal-acid functions. The higher yield to RO products of the S40 and S20 series is in agreement with the lower amount of cis-decalin obtained at the end of reaction. For the bimetallic catalysts on S20 and S40, the yield in RO products increases with the Rh content. For all the monometallic and bimetallic catalysts as well as for the S20 and S40 supports alone, ring-contraction products are also obtained, with similar yields between 3 and 8%. The formation of RC products, not observed on the less acidic S5 support, indicates that the isomerization of decalin proceeds via the acid sites of the S20 and S40 supports. As the formation of RC and RO products occurs only on the catalysts supported on SIRAL with a sufficient acidity, S20 and S40, it can be inferred that whatever the catalyst, the direct ring-opening of decalin is not possible on the metal function, and it proceeds by the hydrogenolysis of ring contraction products obtained by isomerization on the acid sites of the support.

The catalysts supported on S40 have higher yields to cracking products than the catalysts supported on S20 due to the higher acidity of SIRAL 40, in accordance with the lower amount of trans-decalin. These results are in agreement with the general mechanism proposed for the cracking reactions, where the cracking reactions are produced on strong acid sites [60]. Cracking can be minimized with good metal dispersion. It can be seen that in the series S40 the catalysts that have greater metallic dispersion have lower yield to cracking. However, even in the series S20 with similar metallic dispersion values than in S40 series the yield to cracked products is reduced. Cracking products obtained can be attributed only to the acidity of the catalysts; this is evidenced by the absence of these products in the series of supported catalysts SIRAL 5. Moreover, the addition of Pd and Rh, while having no marked effect on the Brønsted acidity, decreases the strength of the acid sites and this inhibits cracking.

The results of Fig. 10 show that the selectivity to RO products of the catalysts supported on SIRAL 40 is approximately 60%, 10% higher than those of the series S20. Although the incorporation of

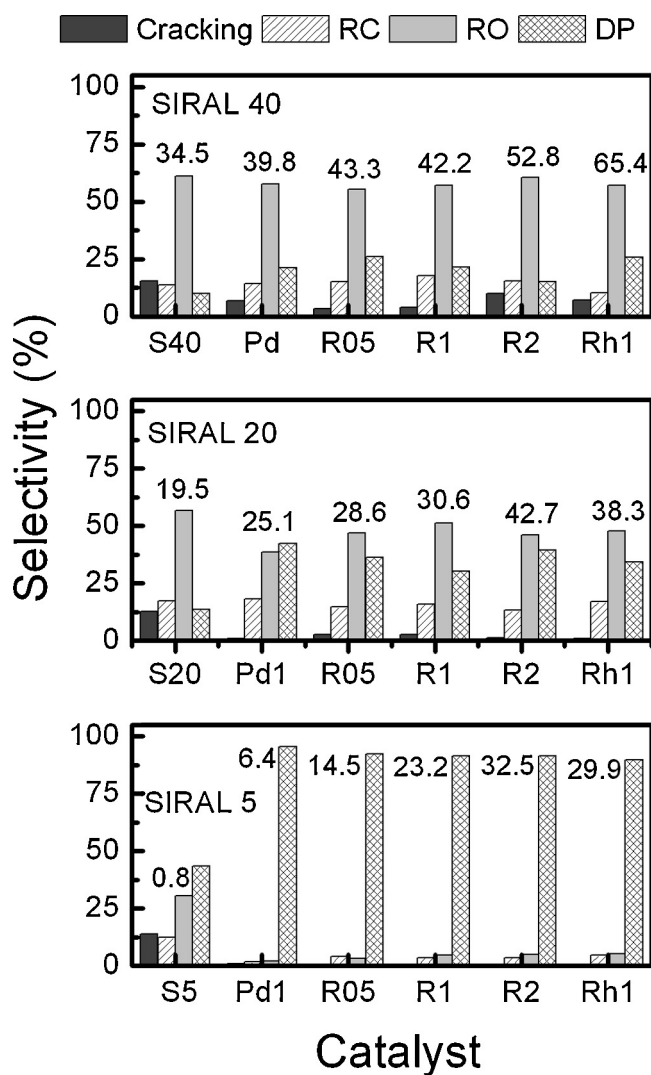


**Fig. 10.** Conversion (value in % given on histogram) and selectivity to cracking, ring contraction (RC), ring opening (RO) and dehydrogenated (DH, including naphthalene.) products after 6 h of decalin transformation at 350 °C.

Pd and Rh can moderate the force of the acid sites, the nature of the support plays an important role. Whereas on S20 and S40 the conversion of decalin increases as the Rh content increases due to the higher hydrogenolytic character of the Rh, the selectivity to RO products seems to strongly depends on the support. It must be underlined that, for the S40 series, the selectivity to RO is similar whatever the catalyst, i.e. for the support alone and the mono and bimetallic catalysts, with a value around 60%, the conversion varying from 34.5 (S40 alone) to 65.4% (Rh1/S40). Thus, for this series the metal function, and more specifically Rh, plays a role in the conversion due to its ability for the hydrogenolysis of ring-contraction products, but the limiting step of the reaction is likely to be the isomerization of decalin to form these intermediate RC products. Again, the influence of the metal charge is more notable in S5 series due to the lower acidity of the support. SIRAL 5 series produces mainly dehydrogenated compounds being their selectivity higher than 90%, since the acidity of the support is not sufficient for the isomerization to RC products, which are the only molecules that can be opened by the metal function. Adding Rh or/and Pd to SIRAL 20 and 40 leads to a decrease of the selectivity to cracking products and an increase of dehydrogenated products. These results can be explained taking into account that the incorporation of Rh or Pd decreases the strength of acid sites (see Fig. 4),

while it increases the total number of acid sites responsible for isomerization reactions. As a consequence the strong acid sites are partially eliminated leading to a decrease of the cracking reactions. The increase of the metal function favors dehydrogenation reactions, and the selectivity to dehydrogenated products increases as the acidity of the support decreases, in the following order: S5 (43–95%)> S20 (30–40%)> S40 (15–25%). Thus, in the presence of the most acidic support (S40), decalin is mainly isomerized to RC products, which are hydrogenolyzed to RO products, whereas on S5, this reaction pathway is not possible and the dehydrogenation is then favored, S20 presenting an intermediate behavior.

#### 4. Conclusions

This work was devoted to the study of mono and bimetallic Pd–Rh catalysts supported on various SiO<sub>2</sub>–Al<sub>2</sub>O<sub>3</sub> (SIRAL 5, 20 and 40) supports, and of the influence of the Brønsted acidity of these oxides on the selective ring opening of decalin.

X-ray diffraction of the SIRAL supports showed typical patterns of amorphous alumino silicate, and SiO<sub>2</sub> and Al<sub>2</sub>O<sub>3</sub> exist in separate phases.

It was found that the total acidity and the Brønsted acid sites of SIRAL series increase with the SiO<sub>2</sub> content. The incorporation of Rh or Pd produces an increase in the total acidity and decreases of the strength of acid sites. The last effect is more makeable as Rh content is increased. 33DM1B isomerization shows that the Brønsted acidity depends strongly on the support (SiO<sub>2</sub> content) and is less affected by the metal charge.

Monometallic Pd catalysts have higher metallic dispersion than the monometallic Rh catalysts. The metallic dispersion decreases as the Rh content is increased for the three bimetallic series.

The support acidity has a strong influence on the conversion and product distribution obtained during the decalin transformation at 350 °C. The catalysts with higher total acidity or Brønsted acid sites have higher yields to RO products. SIRAL 5 series presents low selectivity to RO and high selectivity to dehydrogenated compounds. Adjusting the metal/acid ratio is a key parameter in ring opening reaction. Rh1 or R2 supported on SIRAL 40 combine the Rh ability for hydrogenolysis with amount of Brønsted acid sites appropriate to achieve active and selective catalysts to form ring opening products.

#### Acknowledgements

The authors gratefully acknowledge the “Bernardo Houssay” program for the financial support of this work through a 6 month research grant (Silvana A. D’Ippolito), as well as the SECyT-ECOS program n° A12E02 (2013–2015) which allows continuing the collaboration between the two research teams.

#### References

- [1] B.B.H. Cooper, B.B.L. Donnis, *Appl. Catal. A: Gen.* 137 (1996) 203–223.
- [2] T.C. Kaufmann, A. Kaldor, G.F. Stuntz, M.C. Kerby, L.L. Ansell, *Catal. Today* 62 (2000) 77–90.
- [3] F.G. Gault, *Adv. Catal.* 30 (1981) 1–95.
- [4] G.B. McVicker, M. Daage, M.S. Touvelle, C.W. Hudson, D.P. Klein, W.C. Baird Jr., B.R. Cook, J.G. Chen, S. Hantzer, D.E.W. Vaughan, E.S. Ellis, O.C. Feeley, *J. Catal.* 210 (2002) 137–148.
- [5] H. Du, C. Fairbridge, H. Yang, Z. Ring, *Appl. Catal. A: Gen.* 294 (2005) 1–21.
- [6] J.H. Gary, G.E. Handwerk, *Petroleum Refining Technology and Economics*, Marcel Dekker, Inc., New York, 1994.
- [7] R.C. Santana, P.T. Do, M. Santikunaporn, W.E. Alvarez, J.D. Taylor, E.L. Sughrue, D.E. Resasco, *Fuel* 85 (2006) 643–656.
- [8] H.B. Mostad, T.U. Riis, O.H. Ellestad, *Appl. Catal.* 58 (1990) 105–117.
- [9] H.B. Mostad, T.U. Riis, O.H. Ellestad, *Appl. Catal.* 63 (1990) 345–364.
- [10] L.M. Kustov, A. Yu Stakheev, T.V. Vasina, O.V. Masloboishchikova, E.G. Khelkovskaya-Sergeeva, P. Zeuthen, *Stud. Surf. Sci. Catal.* 138 (2001) 307–314.
- [11] M.A. Arribas, A. Martínez, *Appl. Catal. A: Gen.* 230 (2002) 203–217.
- [12] A. Corma, V. González-Alfaro, A.V. Orchillés, *J. Catal.* 200 (2001) 34–44.

- [13] K. Sato, Y. Nishimura, K. Honna, N. Matsubayashi, H. Shimada, *J. Catal.* 200 (2001) 288–297.
- [14] M.A. Arribas, J.J. Mahiques, A. Martínez, *Stud. Surf. Sci. Catal.* 135 (2001) 303.
- [15] D. Kubička, N. Kumar, P. Mäki-Arvela, M. Tiitta, V. Niemi, T. Salmi, D.Y. Murzin, *J. Catal.* 222 (2004) 65–79.
- [16] D. Kubicka, N. Kumar, P. Maki-Arvela, M. Tiitta, V. Niemi, H. Karhu, T. Salmi, D.Y. Murzin, *J. Catal.* 227 (2004) 313–327.
- [17] M. Santikunaporn, J.E. Herrera, S. Jongpatiwut, D.E. Resasco, W.E. Alvarez, E.L. Sughrue, *J. Catal.* 228 (2004) 100–113.
- [18] M.A. Arribas, P. Concepción, A. Martínez, *Appl. Catal. A* 267 (2004) 111–119.
- [19] G. Crépeau, V. Montouillou, A. Vimont, L. Marey, T. Cséri, F. Maugé, *J. Phys. Chem. B* 110 (2006) 15172–15185.
- [20] E.J.M. Hensen, D.G. Poduval, D.A.J.M. Ligthart, J.A.R. van Veen, M.S. Rigutto, *J. Phys. Chem. C* 114 (2010) 8363–8374.
- [21] B. Pawelec, R.M. Navarro, J.M. Campos-Martin, A. López Agudo, P.T. Vasudevan, J.L.G. Fierro, *Catal. Today* 86 (2003) 73–85.
- [22] S. Nassreddine, S. Casu, J.L. Zotin, C. Geantet, L. Piccolo, *Catal. Sci. Technol.* 1 (2011) 408–4102.
- [23] S. Nassreddine, L. Massin, M. Aouine, C. Geantet, L. Piccolo, *J. Catal.* 278 (2011) 253–265.
- [24] M. Ghiaci, B. Rezaei, R.J. Kalbasi, *Talanta* 73 (2007) 37–45.
- [25] Z. Li, F. Meng, J. Ren, H. Zheng, K. Xie, *Chin. J. Catal.* 29 (2008) 643–648.
- [26] F. Hao, J. Zhong, P.L. Liu, K.Y. You, C. Wei, H.J. Liu, H.A. Luo, *J. Mol. Catal. A: Chem.* 351 (2011) 210–216.
- [27] B. Pawelec, A.M. Venezia, V. La Parola, E. Cano-Serrano, J.M. Campos-Martin, J.L.G. Fierro, *Appl. Surf. Sci.* 242 (2005) 380–391.
- [28] E. Tkalcic, S. Kurajica, J. Schmauch, *J. Non-Cryst. Solids* 353 (2007) 2837–2844.
- [29] C. Leyva, M.S. Rana, J. Ancheyta, *Catal. Today* 130 (2008) 345–353.
- [30] J.T. Feng, H.Y. Wang, D.G. Evans, X. Duan, D.Q. Li, *Appl. Catal. A: Gen.* 382 (2010) 240–245.
- [31] X.L. Seoane, N.S. Figoli, P.C. L'Argentiere, J.A. González, A. Arcoya, *Catal. Lett.* 47 (1997) 213–220.
- [32] A.F. Gusovius, T.C. Watling, R. Prins, *Appl. Catal. A* 188 (1999) 187–199.
- [33] C.W. Chou, S.J. Chu, H.J. Chiang, C.Y. Huang, C.J. Lee, S.R. Sheen, T.P. Perng, C.T. Yeh, *J. Phys. Chem. B* 105 (2001) 9113–9117.
- [34] H. Lieske, J. Völter, *J. Phys. Chem.* 89 (1985) 1841–1842.
- [35] L.S.F. Feio, C.E. Hori, S. Damyanova, F.B. Noronha, W.H. Cassinelli, C.M.P. Marques, J.M.C. Bueno, *Appl. Catal. A* 316 (2007) 107–116.
- [36] J. Valecillos, D. Rodríguez, J. Méndez, R. Solano, C. González, T. Acosta, J. Sánchez, G. Arteaga, *Ciencia* 14 (2006) 125–134.
- [37] L. Rodríguez, D. Romero, D. Rodríguez, J. Sánchez, F. Domínguez, G. Arteaga, *Appl. Catal. A* 373 (2010) 66–70.
- [38] J.I. Villegas, D. Kubička, H. Karhu, H. Österholm, N. Kumar, T. Salmi, D.Y. Murzin, *J. Mol. Catal. A: Chem.* 264 (2007) 192–201.
- [39] D. Kubička, N. Kumar, T. Venäläinen, H. Karhu, I. Kubíčková, H. Österholm, D.Y. Murzin, *J. Phys. Chem. B* 110 (2006) 4937–4946.
- [40] L.M. Kustov, T.V. Vasina, A.V. Ivanov, O.V. Masloboishchikova, E.V. Khelkovskaya-Sergeeva, P. Zeuthen, *Stud. Surf. Sci. Catal.* 101 (1996) 821–830.
- [41] A.K. Aboul-Gheit, S.M. Abodoul-Fotouh, N.A.K. Abodoul-Gheit, *Appl. Catal. A: Gen.* 292 (2005) 144–153.
- [42] A.K. Aboul-Gheit, S.M. Abodoul-Fotouh, S.M. Abdel-Hamid, N.A.K. Abodoul-Gheit, *J. Mol. Catal. A: Chem.* 245 (2006) 167–177.
- [43] J. Valyon, J. Engelhardt, F. Lónyi, D. Kalló, Á. Gömöry, *Appl. Catal. A: Gen.* 229 (2002) 135–146.
- [44] D. Kubička, N. Kumar, P. Mäki-Arvela, M. Tiita, V. Niemi, H. Karhu, T. Salmi, D.Y. Murzin, *J. Catal.* 227 (2004) 313–327.
- [45] V. Nieminen, M. Kangas, T. Salmi, D.Y. Murzin, *Ind. Eng. Chem. Res.* 44 (2005) 471–484.
- [46] A.Yu. Stakheev, L.M. Kustov, *Appl. Catal. A: Gen.* 188 (1999) 3–35.
- [47] C. Kemball, H.F. Leach, B. Skundric, K.C. Taylor, *J. Catal.* 27 (1972) 416–423.
- [48] C.S. John, C. Kemball, R.A. Rajadhayarsha, *J. Catal.* 57 (1979) 264–271.
- [49] H.J. Pines, *J. Catal.* 78 (1982) 1–16.
- [50] J.L. Lemberton, G. Perot, M. Guisnet, *J. Catal.* 89 (1984) 69–78.
- [51] D. Martin, D. Duprez, *J. Mol. Catal. A* 118 (1997) 113–128.
- [52] E.A. Irvine, C.S. John, C. Kemball, A.J. Pearman, M.A. Day, R.J. Sampson, *J. Catal.* 61 (1980) 326–335.
- [53] W. Daniell, U. Schubert, R. Glöckler, A. Meyer, K. Noweckb, H. Knözinger, *Appl. Catal. A: Gen.* 196 (2000) 247–260.
- [54] E.F. Sousa-Aguiar, C.J.A. Mota, M.L. Valle Murta, M. Pinhel da Silva, D. Forte da Silva, *J. Mol. Catal. A: Chem.* 104 (1996) 267–271.
- [55] R.C. Schucker, *J. Chem. Eng. Data* 26 (1981) 239–241.
- [56] W.C. Lai, C. Song, *Catal. Today* 31 (1996) 171–181.
- [57] R. Moraes, K. Thomas, S. Thomas, S. Van Donk, G. Grasso, J.P. Gilson, M. Houalla, *J. Catal.* 286 (2012) 62–77.
- [58] S.A. D'Ippolito, L.B. Gutierrez, C.L. Pieck, *Appl. Catal. A: Gen.* 445–446 (2012) 195–203.
- [59] A. Hass, S. Rabl, M. Ferrari, V. Calemma, J. Weitkamp, *Appl. Catal. A: Gen.* 425–426 (2012) 97–109.
- [60] J.M. Parera, N.S. Figoli, in: G.J. Antos, A.M. Aitani, J.M. Parera (Eds.), *Catalytic Naphtha Reforming Science and Technology*, Marcel Dekker, New York, 1995 (Chapter 3).